Integrative Biology

Accepted Manuscript

ROYAL SOCIETY OF CHEMISTRY

www.rsc.org/ibiology

Insight statement

The *biological insight* is the improved understanding of the role of both the tumor and non-tumor cell components of the tumor stroma and its importance in allowing *in vivo*-like responses to drugs. The *innovation* is the application of microfluidics to facilitate *cis*-coculture, or the culture of non-tumor microenvironmental cell components, without enrichment for a specific cell type, with tumor cells from the same patient, in comparison to monoculture (tumor cells alone). The *integration* of microfluidics and the tumor stroma, MicroC^3, enables the rapid *ex vivo* analysis of therapeutic response of MM patient tumor cells to drug. Using statistical clustering methods, we show here that *ex vivo* responses of MM patient tumor cells to bortezomib strictly correlates with clinical response of the same patients to bortezomib-containing therapies.

Cite this: DOI: 10.1039/c0xx00000x

www.rsc.org/xxxxxx

PAPER

MicroC^3: an *ex vivo* microfluidic *cis*-coculture assay to test chemosensitivity and resistance of patient multiple myeloma cells

Chorom Pak[1,2], Natalie S. Callander[3,4], Edmond W. K. Young[5]†, Benjamin Titz[6,7], KyungMann Kim[4,8], Sandeep Saha[8], Kenny Chng[2], Fotis Asimakopoulos[4], David J. Beebe[4,5], and Shigeki Miyamoto[1,2,4]*

Received (in XXX, XXX) Xth XXXXXXXXX 20XX, Accepted Xth XXXXXXXXX 20XX
DOI: 10.1039/b000000x

Chemosensitivity and resistance assays (CSRAs) aim to direct therapy based upon *ex vivo* response of patient tumor cells to chemotherapeutic drugs. However, successful CSRAs have yet to be developed. Here, we exposed primary CD138$^+$ multiple myeloma (MM) cells to bortezomib, a clinical proteasome inhibitor, in microfluidic-*cis*-coculture (MicroC^3) incorporating patient's own CD138$^-$ tumor-companion mononuclear cells to integrate some of the patients' own tumor microenvironment components in CSRA design. Statistical clustering techniques segregated MicroC^3 responses into two groups which correctly identified all seventeen patients as either clinically responsive or non-responsive to bortezomib-containing therapies. In contrast, when the same patient MM samples were analyzed in the absence of the CD138$^-$ cells (monoculture), the tumor cell responses did not segregate into clinical response clusters. Thus, MicroC^3 identified bortezomib-therapy MM patient responses making it a viable CSRA candidate toward enabling personalized therapy.

Insight statement

The *biological insight* is the improved understanding of the role of both the tumor and non-tumor cell components of the tumor stroma and its importance in allowing *in vivo*-like responses to drugs. The *innovation* is the application of microfluidics to facilitate *cis*-coculture, or the culture of non-tumor microenvironmental cell components, without enrichment for a specific cell type, with tumor cells from the same patient, in comparison to monoculture (tumor cells alone). The *integration* of microfluidics and the tumor stroma, MicroC^3, enables the rapid *ex vivo* analysis of therapeutic response of MM patient tumor cells to drug. Using statistical clustering methods, we show here that *ex vivo* responses of MM patient tumor cells to bortezomib strictly correlates with clinical response of the same patients to bortezomib-containing therapies.

Introduction

In vitro assays able to predict therapeutic response for specific cancer patients would significantly advance efforts towards guiding treatment decisions and enabling individualized therapy. In the past, these assays have been termed Chemotherapy Sensitivity and Resistance Assays (CSRAs) [1–3]. Currently, there are no CSRAs approved for clinical use for any type of cancer [2–4]. There are also technical limitations, such as too low of a tumor cell yield in some patients, inaccessibility of primary tumor cells for other assays, which limit the applicability of CSRAs to patients. Therefore, there is a need for the development of a new type of CSRAs suitable for clinical use, which also overcomes some of the above technical difficulties.

Multiple myeloma (MM) is the second most common hematological malignancy with a median survival of 5-7 years [5–9]. With currently available combination therapies, initial responses to treatment can be as high as 90%. However, patients inevitably relapse and become increasingly refractory to treatment, and the median survival following relapse can be as short as 6-9 months [10,11]. Currently, there are several drug options and combinations to treat MM, including proteasome inhibitors, immunomodulatory compounds, steroids, and DNA damaging agents [12,13]. However, once patients relapse and/or become refractory, it becomes difficult to determine which therapies will be most effective, and quite often treatment is chosen largely on a trial and error basis. Another confounding factor for the choice of therapy is that even the most refractory patients will at times respond to a different drug combination despite previous failed attempts. This results in patients being treated with potentially toxic and ineffective therapy until the "right" drugs are selected. Thus, there is an unmet medical need for novel predictive tools that could guide clinicians to make patient-specific treatment decisions.

It is increasingly evident that the non-malignant cells in the tumor microenvironment also contribute key functions in the maintenance and progression of cancer cells as well as drug resistance [14]. Particularly in the case of MM, there are many cell types in the bone marrow microenvironment, including bone

marrow stromal cells (BMSCs), macrophages, osteoclasts, and other immune cells, which secrete a number of different cytokines and factors known to regulate different signaling

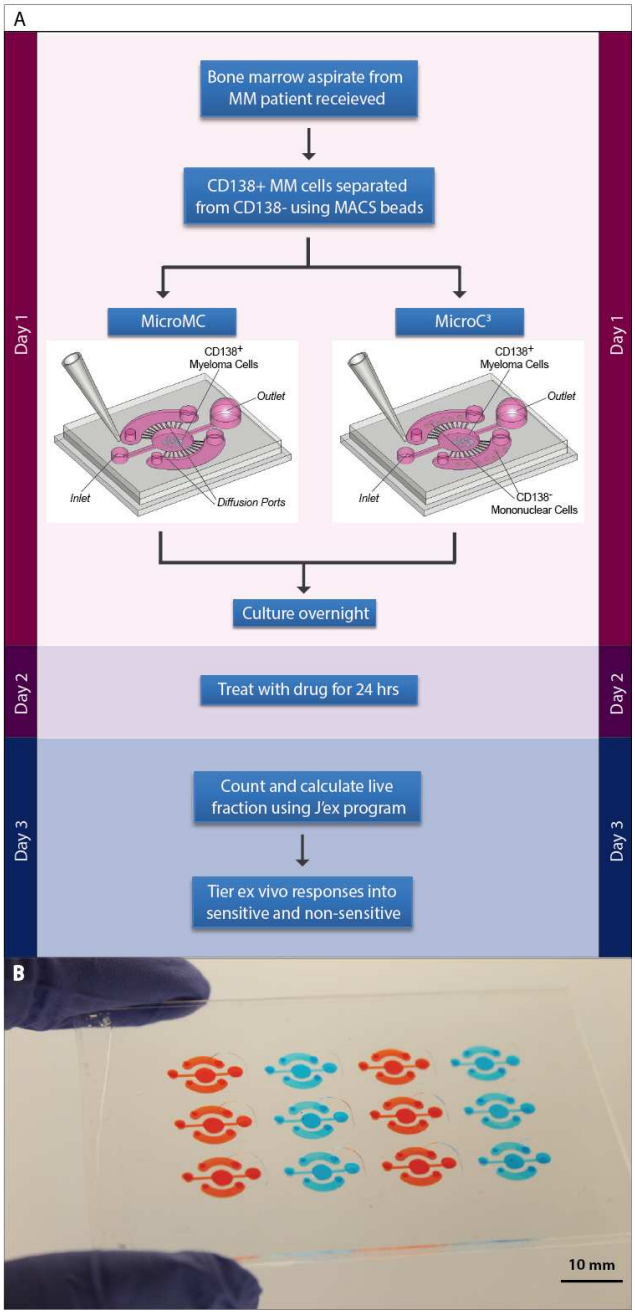

Figure 1. MicroMC and MicroC³. (A) A workflow of MicroMC and MicroC³ is shown. (B) A 4x3 array of microfluidic channels used for both MicroMC and MicroC³ is shown.

pathways that may contribute to chemotherapy resistance in MM [14–18]. Moreover, cell-cell contacts can provide additional layer of protection toward MM cells [19,20]. In order to incorporate tumor microenvironment in *in vitro* assays, efforts are underway, including organoid assays and xenograft assays using primary patient samples, which may take such other non-tumor cell components into consideration for therapy-predictive assay development [21–24].

Culture platforms utilizing microfluidics are gaining prominence because of their ability to measure cell behavior and function at single cell levels [25–28], allowing valuable information to be garnered from low starting material while at the same time enabling more experimental conditions. Particularly with the advent of newer technologies, such as passive pumping and paper-based microfluidics, microfluidic devices have become more easily adapted for use by biologists, requiring only standard tools found in most biology labs [29,30]. Tumor cell yield obtained from MM bone marrow biopsies can widely vary (less than 10^4 to more than 10^7 cells per biopsy sample); samples with low tumor cell yields may be difficult to analyze with conventional methods of coculture (i.e., Transwell®). Moreover, extramedullary myeloma tissue sampling often yields lower amounts of tumor cells than standard bone marrow biopsy-derived material. Previously we reported the development of a microfluidic culture platform that enables culturing and functional analysis of low numbers of suspension cells, such as blood cancer tumor cells, in coculture with other cell types placed in different compartments permitting communication through soluble factors via diffusion ports [31].

Here we report the development of a CSRA based on the above microfluidic system using patients' bone marrow $CD138^+$ malignant plasma cells and $CD138^-$ cells referred to here as MicroC³ (microfluidic *cis*-coculture). The unique design feature of MicroC³ is that it allows the *ex vivo* measurement of responses of primary suspension MM cells to therapeutic drugs in the presence of paired non-tumor cell types derived from the same patient marrow biopsies (*cis*-coculture). This design is thus conceptually and functionally distinct from previous CSRAs in three ways. First, previous CSRAs employed cancer cells in isolation, i.e., in monoculture. Second, prior attempts to coculture primary tumor cells with other cell types are typically performed in *trans*-coculture, or coculture of tumor cells and other cell types isolated from different patients [15,22,32] or stroma-derived cell lines, e.g., HS-5. Lastly, while many previous CSRAs required culturing and expansion of the patient tumor cells *in vitro*; MicroC³ is performed *ex vivo* and is completed within 3 days (after bone marrow biopsy). The potential utility of MicroC³ was tested by measuring the *ex vivo* toxicity responses of MM tumor cells in MicroC³, versus the comparison group cultured in microfluidic monoculture (MicroMC) in the absence of cocultured non-tumor cell types, to varying doses of a clinical proteasome inhibitor, bortezomib [10,33]. We then correlated these *ex vivo* responses of MM cells to clinical responses of those patients to bortezomib-containing therapies. We show that according Gaussian mixture model clustering, while *ex vivo* patient MM cell responses from 11 of 15 patients correlated to respective patient clinical responses in MicroMC, those of 17 of 17 patients matched their respective clinical responses using MicroC³. Thus, MicroC³ was able to identify clinical responses of all patients exposed to therapies containing bortezomib.

Results

MicroMC and MicroC³ operation and cytotoxicity analysis

The microfluidic microchannel system we had previously

reported [31] was employed in this work to investigate its utility in the analysis of primary MM patient samples. In short, by leveraging pressure differences at differently sized inlet and outlet ports, this platform is operated by passive pumping [29],

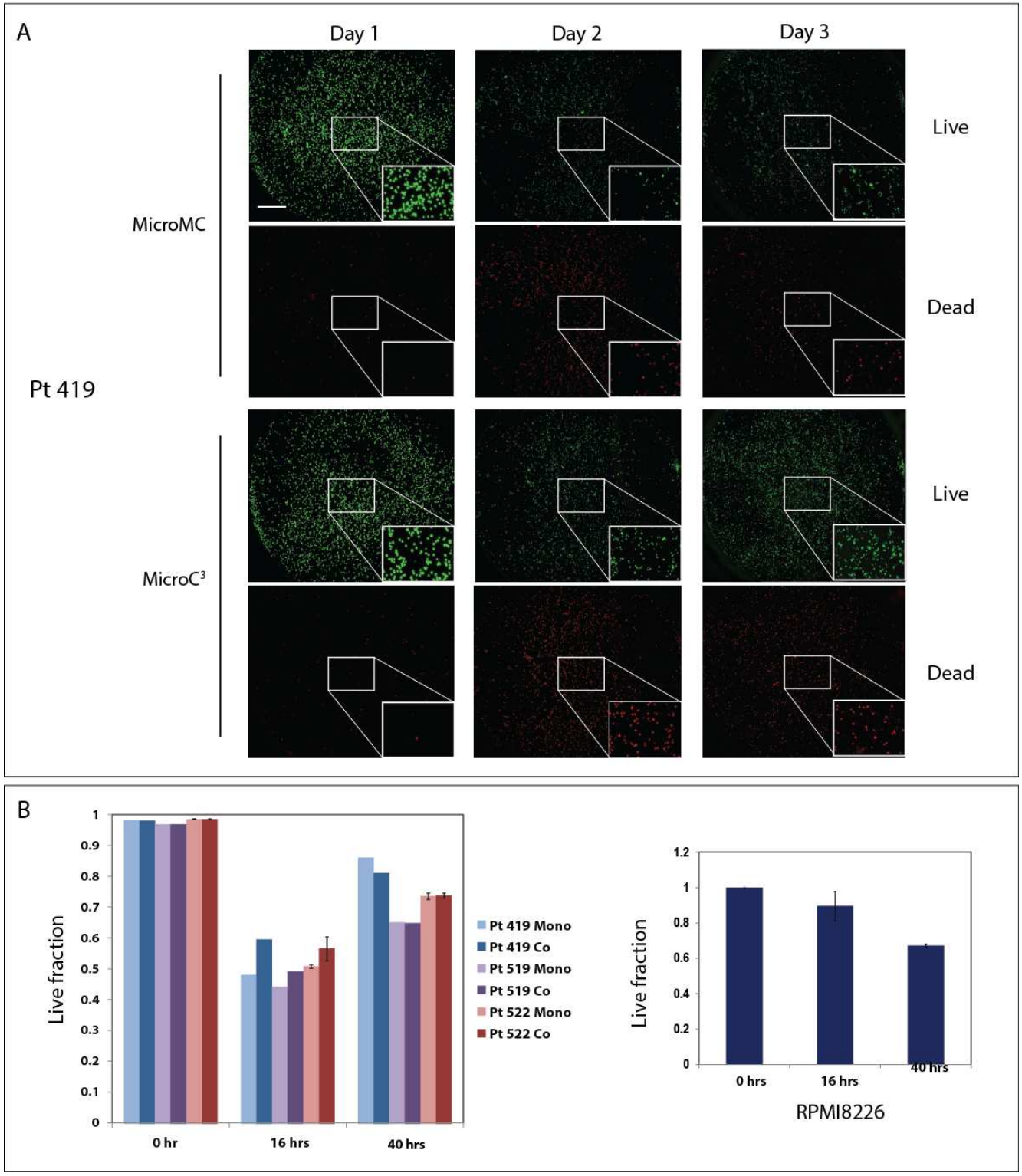

Figure 2. MM cell survival in MicroMC and MicroC³. (A) Images of Pt. 419, 519, and 522's MM cells within the central well in mono- and *cis*-coculture at 0, 16, and 40 hours. MM cells were stained with calcein AM and ethidium homodimer and imaged. Insets show magnification of the selected area. (B) Left graph: Live fractions calculated from the live and dead cells from Figure 2A for both mono- and *cis*-coculture. Error bars indicate SD from technical replicate of n=3. Right graph: Live fractions calculated for RPMI8226 cell survival within the microchannelat 0, 16, and 40 hours.

Cite this: DOI: 10.1039/c0xx00000x

www.rsc.org/xxxxxx

PAPER

Table 1. MM patient characteristics and clinical status.

	Patient number	Age	Sex	ISS stage	High Risk	Albumin (g/L)	Beta-2 (mg/L)	Cytogenetics	FISH	Bone disease	IFE	CD138+ cell count	Previous treatment	Status at BMBX	% plasma	Next treatment
BMBX pre bortezomib therapy	314	68	M	nd	nd	nd	nd	nd	nd	nd	nd	1,510, 000	VRD	Sensitive	nd	VRD (PD)
	316	63	F	I	no	4.3	3.3	nd	t(11;14)	yes	kappa	1,580,000	RD	Refractory	33%	VRD (PR)
	317	73	M	III	yes	2.3	8.1	hypodiploid,-13	t(11;14)	yes	lambda	9,800,000		Newly diagnosed	90%	VD (PR), ASCT, R, VRD (DOD)
	318	51	F	III	no	3.8	7.2	nd	-13	no	kappa	360,000		Newly diagnosed	10%	V (CR)
	323	61	F	II	yes	2.7	4.5	nd	p53	yes	IgG lamda	2,100,000		Newly diagnosed	40%	VRD (PR), ASCT, R
	345	68	M	I	no	3.8	1.9	t(11;14)	t(11;14)	yes	IgG kappa	1,500,000	RD, VAD, ASCT	Sensitive	26%	VRD (PR), CyBorD (PR)
	402	68	M	III	yes	3.1	32	-13	t(14;16)	no	IgA lambda	200,000	RD, VD, C, ASCT, M, V, C, M, R	Refractory	10%	VRD (PD, DOD)
	442	85	F	III	no	3.1	6.5	nd	t(11;14)	yes	IgG kappa	14,000,000		Newly diagnosed	61%	CyBorD (SD), RD (PR)
BMBX post bortezomib therapy	329	65	M	II	no	nd	nd	hyperdiploid	p53	yes	IgA kappa	2,820,000	RD, ACT, RD, VRD, CRD	Relapsed/Refractory	28%	RD (PR)
	330	58	M	nd	nd	nd	nd	nd	nd	yes	IgG kappa	600,000	VAD, ASCT	Relapsed	50%	R (PR)
	353	66	M	III	nd	nd	8.6	t(11;17)	nd	yes	IgA kappa	8,800,000	VRD, Benda, Pom, V, M	Refractory	100%	Carf (PD, DOD)
	398	62	M	I	no	3.6	3.8	-20	normal	nd	nd	2,400,000	D, Rad, VRD	Relapsed	10%	ASCT, CDA, CarfD (PD, DOD)
	419	76	F	I	no	4.1	2.9	nd	nd	yes	IgA kappa	8,600,000	VRD, ASCT	Relapsed	40%	RD (PR)
	431	73	M	III	yes	4	8.1	-13	t(11;14)	yes	lambda	7,300,000	VRD, C, M, VRD	Refractory	80%	(PD, DOD)
	432	53	M	II	no	3.3	5.24	hyperdiploid	nd	yes	IgG kappa	420,000	VRD, ASCT	Sensitive	12%	RD (PR)
	435	73	M	amyloid	nd	nd	nd	nd	t(11;14)	nd	nd	560,000	CyBorD	Sensitive	3%	RD
	446	67	M	II	no	4	nd	nd	nd	yes	IgA kappa	13,700,000	RD, V, Carf	Relapsed/Refractory	46%	C (PR), VRD, ASCT
	447	55	M	II	no	3	4.8	nd	nd	yes	IgA kappa	660,000	VAD, RD	Relapsed	1%	ASCT

ISS, international staging system; Beta-2, beta-2 microglubilin; FISH, fluorescence in situ hybridization; IFE, immunofixation electrophoresis; BMBX, bone marrow biopsy; A, adriamycin; ASCT, autologous stem cell transplant; Benda, bendamustine; Carf, carfilzomib; CyBorD, cyclophosphamide, bortezomib, dexamethasone regimen; C, cyclophosphamide; D, dexamethasone; M, Melphalan; Pom, pomalidomide; Rad, radiation; R, Revlimid; T, thalidomide; V, Velcade; CR, complete response; DOD, died of disease, PD, progressive disease; PR, partial response; SD, stable disease; nd, no data.

requiring only a micropipet for operation. Suspension cells are seeded through the inlet port of the central well and are allowed to settle overnight (Figure 1). Other cell types used for coculture studies are seeded through the inlet ports of the side chambers. This system incorporates the following features: 1) capacity to be performed for virtually all MM patients (i.e., 7500 cells per endpoint in the current study), 2) both tumor and non-tumor cells incorporated to mimic certain aspects of *in vivo* microenvironment, and 3) simple and quick to perform without the need for extensive growth of the cells *in vitro*.

The entire assay requires 3 days to complete. On Day 1, after bone marrow aspiration, $CD138^+$ tumor cells were sorted (within 24 hours of aspiration) and cultured in either *mono-* (MicroMC) or *cis*-coculture with the patients' own $CD138^-$ non-tumor mononuclear cell fractions ($MicroC^3$) (Figure 1). In the past, *cis*-coculture with a patient's own tumor and non-tumor cells, such as BMSCs, could only be accomplished from the individual bone marrow aspirate samples by cryopreservation of the MM tumor cells until BMSCs were established. This was necessary because MM tumor cells are only viable for about 3 to 10 days *ex vivo*, while BMSCs take about 2 weeks to establish [34,35]. However, we discovered that cryopreservation of MM tumor cells resulted in a great loss of viability of patient cells, with an average of ~25% of cells being viable after thaw (Table S1), potentially skewing the results gained subsequently. Therefore, cryopreservation of MM tumor cells was avoided in the current study and all patient samples were analyzed fresh. To minimize an artificially magnified contribution of a specific non-tumor cell type, such as BMSCs or macrophages, and to preserve the relative contribution of other non-tumor cell types present in each patient biopsy, we placed the entire mixture of $CD138^-$ cells in the side chambers of $MicroC^3$ assay. The separation of $CD138^+$ cells and $CD138^-$ cells into distinct chambers enabled the unambiguous determination of the drug impacts on MM cells. Thus, while this assay permits the analysis of soluble interactions between MM cells and non-tumor companion cells from each biopsy sample, it does not account for potential effects mediated by direct contacts between MM cells and non-MM cells.

After a 16 hour culturing period (necessary to retain >99% of cells in central well), the tumor cells were treated with varying doses of bortezomib, ranging from 0 to 300 nM (calculated final concentrations) for 24 hours (Figure 1) (Days 2 – 3). Due to the limited number of tumor cells obtained, some patient samples could not be analyzed for all bortezomib doses. The $CD138^+$ cells were then stained with calcein AM and ethidium homodimer to stain for live and dead cells, respectively, as we have done previously [31]. Live and dead cells were counted using an ImageJ-based in house software program (J'experiment) [31]. Live fractions for each dose were calculated and normalized to the 0 dose bortezomib controls for both MicroMC and $MicroC^3$. Initial analysis of the viability of primary MM cells obtained from several biopsies within the contexts of MicroMC and $MicroC^3$ measured at the times corresponding to seeding (0 hr, Day 1), prior to drug treatment (16 hr, Day 2), and after drug treatment

Cite this: DOI: 10.1039/c0xx00000x

www.rsc.org/xxxxxx

PAPER

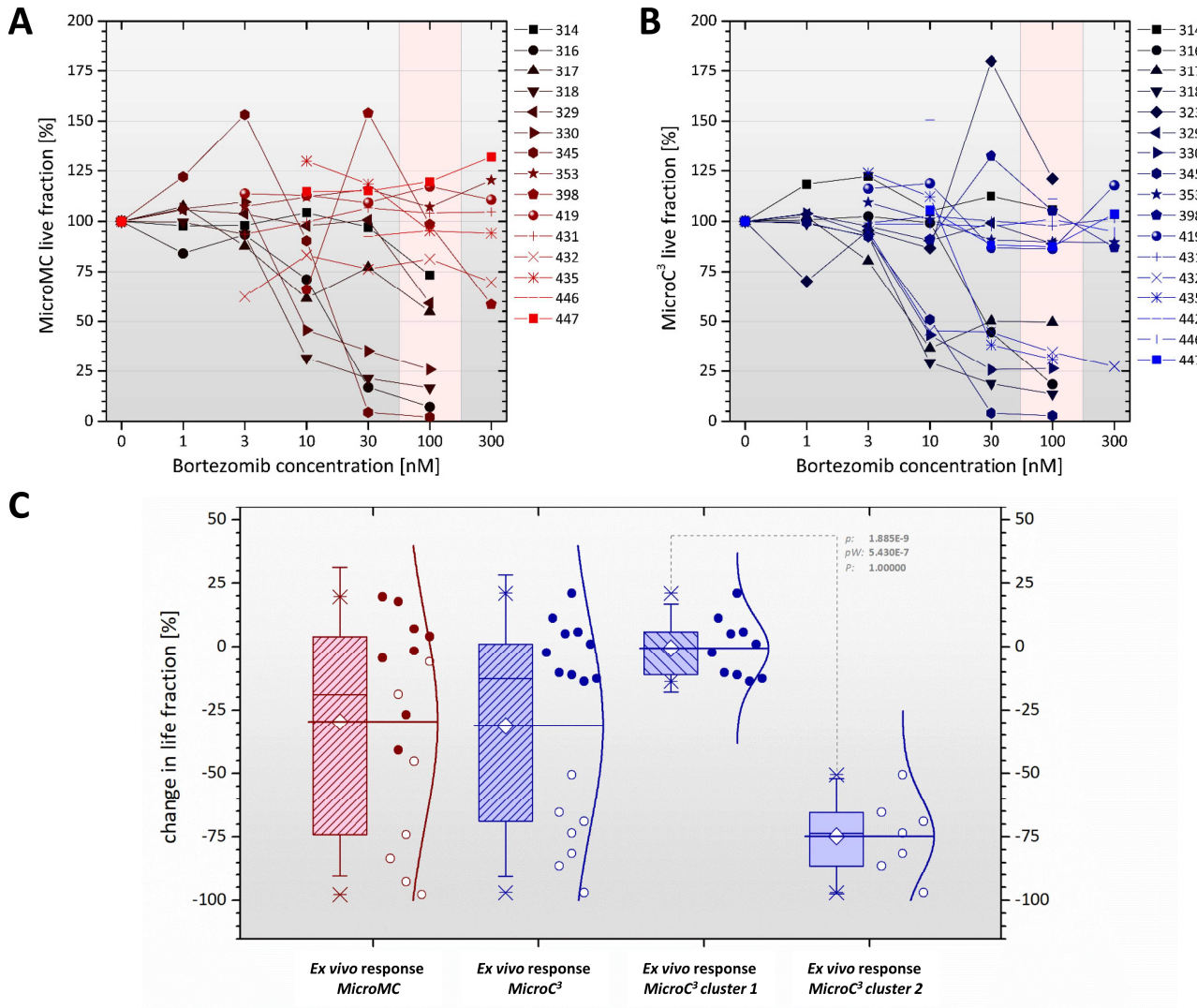

Figure 3. *Ex vivo* responses of patient MM tumor cells to bortezomib. (A) *Ex vivo* responses patients' MM cells in MicroMC to bortezomib are shown. (B) *Ex vivo* responses of patients' MM cells in MicroC^3 to bortezomib are shown. C) Box plots showing patient MM tumor cells' *ex vivo* responses to bortezomib compared between MicroMC (MC, shown in red) and MicroC^3 (shown in blue) (x-axis). The live fraction change is compared between the 0 dose and 100 nM dose of bortezomib (y-axis). Open symbols denote clinically responsive patients to bortezomib-containing therapies whereas solid symbols indicate clinically non-responsive patients. CC clusters 1 and 2 of patient *ex vivo* responses in MicroC^3 to bortezomib are shown as two separate box plots (blue).

(40 hr, Day 3) in the absence of drug treatment (Figure 2A) indicated that the viability of MM cells at different time points was comparable among patients (Figure 2B) and to that of a MM cell line, RPMI8226 (Figure 2C). To maximize the yield of drug response trend of MM cells from individual patient samples, we chose to perform dose-response analysis instead of technical replicates at an arbitrary dose. Some technical replicates were performed only when the MM cell yield was sufficient for such studies (Figures S2 and S3).

Distribution and statistical clustering analysis of ex vivo patient MM cell responses

The % fractions of surviving MM cells in response to increasing doses of bortezomib in MicroMC and MicroC^3 for patient samples analyzed are shown in Figures 3A and B, respectively. The patient characteristics are presented in Table 1. To understand the relationship between effective concentrations of bortezomib over time in the microchannels and those reported

in patients [36,37], we incubated 100 nM bortezomib for different times and measured the ability of remaining bortezomib in the media to inhibit the proteasome activity present in RPMI8226 MM cells by performing the Proteasome-Glo Assay (see Materials and Methods section). From these values, we extrapolated the relative concentrations of bortezomib present in microchannels over time and found approximately 0 nM at 12 hrs and later. The calculated area under the curve (AUC) amount of bortezomib for the 100 nM dose incubated over 24 hours in microchannels was 112.92 ng*h/mL (Figure S1). The plasma concentration of bortezomib peaks between 50 to 200 nM and drops off sharply when administered intraveneously or a slightly slower following subcutaneously injection [36,37]. Nevertheless, the AUC was reported to be comparable between the two administrative routes being ~70 to 150 ng*h/mL. Thus, our data suggested that the addition of 100 nM bortezomib in microchannels exposed MM cells with AUC profiles approximating those seen in patient plasma.

Subsequently, the percent changes in live fraction of MM cells from the 0 nM to 100 nM dose of bortezomib in MicroMC and MicroC^3 for all patients were calculated. Figure S2 shows the results with technical variations wherever available. Patients 323 and 442 were omitted from MicroMC group since their MM cells did not survive in MicroMC; however, they were included in MicroC^3 analysis as their MM cells survived in MicroC^3. When these results were plotted in box plots, MicroC^3 responses appeared to segregate into two groups, while responses within MicroMC did not (Figure 3C, left two plots). To further investigate the existence of different clusters of MM cell responses in microchannels, both the AIC (Akaike Information Criterion) and BIC (Bayesian Information Criterion) were calculated for unimodal, bimodal, and trimodal distributions for both MicroMC and MicroC^3. For MicroC^3, a bimodal distribution of the response data was favored by the AIC as well as the BIC over unimodal and trimodal distributions (Table S3). In contrast, none of these distributions was favored by AIC or BIC for MicroMC responses.

As both the AIC and BIC values indicated that a bimodal distribution was favored for MicroC^3, *k*-means and Gaussian mixture clustering methods were applied to segregate MicroC^3 *ex vivo* responses. The *k*-means and Gaussian mixture clustering analyses segregated 17 *ex vivo* responses in MicroC^3 into two clusters: 1 – non-sensitive (10 cases), 2 – sensitive (7 cases) (Table S3). The separation of the two resulting clusters ($p < 10^{-5}$) (Figure 3C, right two plots) was further in line with the Otsu threshold independently derived for the same data (Figure S2).

Correlation of ex vivo MM cell drug responses to clinical responses of corresponding patients

The *ex vivo* responses within MicroMC and MicroC^3 were next compared with the clinical responses of the same patients. The top half of Table 1 lists patients whose bone marrow biopsies were collected prior to bortezomib-containing therapy; while the bottom half lists patients whose bone marrow aspirates collected post bortezomib-containing therapy. According to IMWG criteria, patients were deemed to be responsive if they had a partial response (PR) or greater and refractory or non-responsive if they had stable disease, progressive disease, relapsed and/or become refractory [38]. For patients whose bone marrow aspirates were collected prior to therapy, their clinical responses were determined by response to their next bortezomib-containing therapy. For patients whose samples were collected post therapy, their clinical responses were determined by current status at the time of biopsy. All samples were collected and analyzed *ex vivo* without the prior knowledge of patients' clinical history to eliminate operator bias. The clinician determining responses was also blinded of the *ex vivo* response data.

Remarkably, the MicroC^3 clusters separated by *k*-means and Gaussian mixture clustering into non-sensitive and sensitive were correctly identified as either clinically non-responsive or responsive, regardless of whether the aspirate was acquired prior to or post bortezomib-containing therapy (Figure 3C, right plots, Table S3). In contrast, only 12/15 (7/8 non-sensitive and 5/7 sensitive) of MicroMC responses (Figure S5) matched the patients' respective clinical responses (Table S3) based on *k*-means clustering. The two patients (Pt. 323 and 442) whose samples were not included in the MicroMC group were both newly diagnosed and were clinically responsive and nonresponsive, respectively. According to Gaussian mixture clustering, 11/15 (6/8 non-sensitive and 5/7 sensitive) MicroMC responses matched their respective clinical responses (Table S3). Similar results were obtained when the clustering methods were applied to the changes in live fraction from 0 to 30 nM of bortezomib treatment. MicroC^3 identified 16/16 *ex vivo* responses, while MicroMC identified 12/15 at this dose of bortezomib (Table S3, bottom panel). Thus, patients' CD138$^+$ MM cells in MicroC^3 appear to more uniformly cluster into sensitive or non-sensitive according to the patients' clinical responses compared to the same cells analyzed alone without the influence of CD138$^-$ tumor-companion cell population.

One anomalous patient, Pt 402, was removed from the above analyses. Pt 402's CD138$^+$ cells showed increased survival in the presence of bortezomib *ex vivo* in MicroC^3 (but reduction in MicroMC) (Figure S5) and this patient's clinical response was non-responsive. However, when included in the clustering analyses, trimodal distributions were favored with the Pt 402's *ex vivo* response being classified as a third cluster (Table S4). Thus, while his *ex vivo* response in MicroC^3 (but not in MicroMC) matched his clinical response, Pt 402 was removed as a statistical anomaly. Peculiarly, Pt 402 was the only patient with a t(14;16) translocation affecting c-Maf oncogene with a very poor prognosis that occurs in ~5% of MM patients [39–41].

MicroC^3 ex vivo responses and patient clinical responses to future bortezomib-containing therapy

Pt's 317, 318, and 323 were newly diagnosed patients and their tumor cell responses were classified as sensitive to bortezomib in MicroC^3 assay (Figure 3). These patients then went on bortezomib-containing regimens without the clinician's prior knowledge of the *ex vivo* responses (Table 1, bottom half). Clinically, Pt. 317 and 323 had a partial response, and Pt. 318 showed a complete response to bortezomib-containing regimens. Similarly, Pt. 316 was classified as refractory to treatment with lenalidomide and dexamethasone at the time of the biopsy (Table 1) but the patient's tumor cell response to bortezomib in MicroC^3 assay at biopsy was classified as sensitive (Figure 3). This patient

then went on a bortezomib-containing therapy and had a partial response. In contrast, Pt. 442 was a newly diagnosed patient whose tumor cells were classified as bortezomib non-sensitive in MicroC^3 assay (Figure 3). This patient then went on a bortezomib-containing regimen, again without the clinician's prior knowledge of the *ex vivo* data, and did not respond clinically. Therefore, these patients' CD138$^+$ cell response to bortezomib in the MicroC^3 system correlated with the patients' future clinical response to bortezomib-containing therapy.

Discussion

A predictive CSRA that enables stratification of patients prior to specific therapy would allow patients to avoid ineffective therapies as well as unnecessary cost associated with such therapies. In the present study, we have developed and tested MicroC^3, a microfluidics-based *cis*-coculture CSRA, which incorporates several new features into an *ex vivo* predictive assay platform while being accessible to researchers without the need for highly sophisticated technical capabilities. First, both tumor and non-tumor cells from the same patients are incorporated to capture tumor and non-tumor cell heterogeneity in individual patient samples. Second, the MicroC^3 analyzes only thousands of CD138$^+$ cells per condition, thereby making it applicable to virtually all MM patients. And finally, the MicroC^3 assay operation is simple and takes only three days from the sample acquisition to the analysis of the cell responses, negating the need for extended culturing and passaging of the patient cells, which could alter their phenotypes. Significantly, MicroC^3 CSRA segregated *ex vivo* patient tumor cell responses to bortezomib into two clusters, which correctly identified patients' clinical responses to bortezomib-containing therapies.

Our previous and others' studies suggested that both non-tumor cells, such as BMSCs and macrophages, and MM cells from individual patients display considerable heterogeneity in signaling responses and functions[32,16,18,15]. To incorporate both tumor and non-tumor cell heterogeneity in the design of *in vitro* toxicity assay, we avoided artificial enrichment of a specific cell population, such as BMSCs or macrophages, and associated bias of functional contributions via soluble factors produced by them[15,42]. Bortezomib can also exert effects on non-tumor cells within the MM tumor microenvironment, in addition to direct effects on MM cells [14–16,43,44]. Thus, incorporation of total CD138$^-$ cell population in MicroC^3 likely enabled *ex vivo* recapitulation of key aspects of tumor microenvironment [14,45–48] distinguishing it from traditional monoculture designs used in previous CSRAs [1–3].

Another critical feature of MicroC^3 is the microscale analysis of patient MM cell toxicity. The low fluid volumes may concentrate important soluble factors produced by both the tumor and non-tumor companion cells which may otherwise be diluted in conventional culture conditions (e.g., Transwell cultures). Other studies have also suggested that these and other inherent properties of microfluidic culture, including lack of convection and transport by diffusion, lead to an improved simulation of the tumor microenvironment [26,49,50]. Though the inclusion of the tumor microenvironment components in microscale assays is becoming increasingly popular - and powerful - through the development of cells-, tissues-, and organs-on-chips [51–53], as well as the patterning of different cell types and microfluidic Campenot chambers [51,52,54], MicroC^3 is the first reported assay system in which suspension cancer cells in coculture with different cell types from the same patient are analyzed together.

While all other previous CSRAs categorized patients into high and low response groups, we incorporated clustering methods to segregate *ex vivo* patient responses in MicroC^3. Separate clusters segregated by these statistical methods have successfully identified all 7 and 10 patients who were clinically responsive and non-responsive, respectively, to bortezomib-containing therapy. In contrast, MicroMC responses did not cluster as above despite a large percentage of informative cases (11/15, 73%, according to Gaussian mixture modeling) matching clinical responses. When the two failed cases were included, MicroMC results (11/17, 65%) were still comparable or better than other CSRAs tested for other cancer types that have garnered ~30-60% accuracy [1,55,56]. Thus, while MicroMC may also be useful, MicroC^3 particularly merits further evaluation as a potentially useful CSRA for predicting clinical MM disease responses.

While these responses of MM cells to bortezomib in MicroC^3 are encouraging, its applicability as a CSRA requires further studies and improvements. First, a prospective clinical study with appropriate statistical power is needed to determine the extent of predictability of the MicroC^3 assay for future clinical bortezomib responses. We chose to focus initially on bortezomib because it is one of the most commonly used drugs in MM therapy combinations; it is used to treat both newly diagnosed and relapsed/refractory MM patients[33,57,58]. Owing to the clinical success of bortezomib, other proteasome inhibitors have been approved (carfilzomib) or are in development (oprozomib, ixazomib)[59,60]. In addition, bortezomib is also approved for the treatment of another blood cancer, mantle cell lymphoma[61].Second, studies are required to test if MicroC^3 could also be useful for other, as well as combinations of, therapeutic agents, such as lenalidomide and pomalidomide (immunomodulatory drugs, IMiDs). Although IMiDs have been suggested to exert their effects through modulation of the immune cells, a recent study suggested a mechanism of cell death induced by these drugs through Cereblon-mediated degradation of Ikaros proteins [62–66]. Third, MicroC^3 currently does not incorporate drug resistance of MM cells mediated by adhesion to the ECM or with certain non-tumor cells, such as BMSCs and macrophages [20,67], and modifications to accommodate such a mechanism may lead to an improved CSRA platform. To accommodate this change in the future, one could simply add matrix or tumor and non-tumor cells together in the central well. Fourth, an additional study could test if MicroC^3 is also amenable to analysis of extramedullary myeloma that is also infiltrated by non-tumor cells, such as macrophages [16], using patients' blood samples. Fifth, the MicroC^3 assay should also be tested with other hematological malignancies [31], particularly those that support sampling of both tumor cell and non-tumor cells. Finally, MicroC^3 can be configured into a high throughput format with alternative device materials (such as polystyrene), robotic automation to minimize operator bias, and improved accuracy of sample handling and data acquisition. While other efforts are also underway by employing mono- and coculture systems (e.g.,

ex vivo 3-D RCCS™ bioreactor) [21], *in vivo* xenograft models (e.g., humanized mouse models) [22,68–70], and patient-derived xenograft (PDX) models [71] to capture aspects of the patients' tumor microenvironment, further improvements in the MicroC^3 platform could provide a readily accessible, automated, and high-throughput CSRA for hematological malignancies.

Materials and Methods

Microchannel fabrication and preparation

Single-use devices comprised of 12 or 24 cell culture chambers were fabricated using soft lithography using two master molds established previously [72,73]. Polydimethylsiloxane (PDMS) was mixed at a 10:1 base:curing agent ratio, poured on the master molds, and cured at 80°C for 4 hrs. Two separate PDMS layers were made, one for the channel layers containing the central well, side chambers, diffusion ports, and inlet and outlet channels, and one for the access port layer. The two PDMS layers were then soxhlet extracted and plasma treated to bond to a glass slide. The final device was then baked at 120°C for 15 min to increase bond strength and release any bubbles.

Before cell culture, the chambers on the device were filled first with 70% ethanol as a wetting agent as well as a disinfectant. The ethanol was rinsed with 3 volume replacements (VRs) of 1X phosphate-buffered saline (PBS). The 1X PBS was then replaced with 3 VRs of the appropriate cell culture medium. The final such prepared device could be stored up to 3 weeks in a 37°C incubator when encased with appropriate humidifying and sterile conditions. When stored longer than 24 hours, the media was replaced with 1 VR of fresh media prior to cell seeding.

Cell line culture and preparation

RPMI8226 (human MM cell line) was obtained from ATCC. RPMI8226 cells (1.0 to 1.5 x 10^5 cells/mL seeding density) were routinely cultured at 37°C with 5% CO_2 in high-glucose Dulbecco's modified eagle's medium (DMEM) containing 10% fetal bovine serum (FBS), 100U/mL penicillin, 100g/mL streptomycin (1% P/S), and 10mM hydroxyethyl piperazineethanesulfonic acid (HEPES) in tissue culture-treated flasks. Cells were passaged every 2 to 3 days. For experiments conducted in microchambers, RPMI8226 cells were collected and resuspended at 1.0x10^6 cells/mL of fresh growth media. A total of 5µL of the concentrated cell suspension was dispensed by passive pumping into each microchamber.

Primary patient cell culture and preparation

Bone marrow aspirates (5-10ml each) were obtained with informed consent from patients diagnosed with multiple myeloma at the University of Wisconsin-Madison Hospital in accordance with University of Wisconsin-Madison Institutional Review Board requirements (HO0-7403 protocol). Clinical status of the patients was determined by International Myeloma Working Group (IMWG) criteria [38]. 'Sensitive or Responsive' is defined as patient achieving at least a partial remission/response. 'Relapsed' is defined as patient having $\geq$ 0.5g/dl increase in monoclonal protein or >200mg in 24 hours in urine light chains after obtaining at least a partial remission. 'Refractory or Resistant' is defined as patient having progressed on or within sixty days of treatment. Relapsed and/or refractory patients were defined as non-responsive patients for the purpose of this assay. The researcher assessing clinical statuses of the patients was blinded to assay results and separate from the staff performing the assay. The *ex vivo* data and the clinical statuses were only compared after the assay was completed.

Aspirate volumes were doubled with Iscove's Modified Dulbecco's Medium (IMDM) + 100 units/mL heparin (Sigma-Aldrich). They were doubled again with IMDM + 10 units/mL DNAseI (Roche). After rocking at room temperature for 30 minutes, 2 volumes of cell mixture were put over 1 volume of lymphocyte separation medium (Cellgro) and centrifuged for 35 minutes at 200g. The interface and 2-3mLs of the buffy coat layer were taken, and rinsed with PBS + 2mM ethylenediaminetetraacetic acid (EDTA). At this point, the total mononuclear cells were either sorted or cryopreserved with cryopreservation medium (90% FBS, 10% DMSO). $CD138^+$ magnetic MACS® beads (Miltenyi Biotec) were used to positively sort for multiple myeloma cells per the manufacturer's instructions to >95% purity as determined by fluorescence-activated cell sorting (FACS). For sorting with cryopreserved samples, the sample was quickly thawed at 37°C, resuspended in 10 mL of DMEM and 20% FBS and pelleted to remove DMSO. The sample was then incubated in high glucose DMEM containing 20% FBS and 1% P/S and 10mM L-glutamine with the addition of DNAseI for 1 hour with agitation approximately every 15 min to break up cell clumps. The sorting protocol was then followed as above with the $CD138^+$ MACS beads.

For microchannel experiments, $CD138^+$ cells were resuspended in high glucose DMEM containing 20% FBS and 1% P/S and 10mM L-glutamine at a density of 1.5x10^6/mL and 5µL were seeded into the inlet port of each central well for a total of 7500 cells. For coculture experiments, $CD138^-$ cells were resuspended at a density of 4x10^6 cells/mL in the same media as the $CD138^+$ cells and 2uL were seeded into the inlet port of each side channel for a total of 8000 cells on each side. After an overnight culture, fresh media containing varying concentrations of drug were added to the input port, resulting in exposures of both MM cells and non-MM cells in the side chambers at the final concentrations needed. If the number of cells permitted, duplicates of drug dose conditions were performed. Cultures were treated with the drug for 24 hrs after which live and dead cells were stained, respectively, as described below.

Reagents

Bortezomib (PS-341 or Velcade) was obtained as a 2.6mM clinical saline solution from Millenium Pharmaceuticals and stored at -80°C in separate aliquots. The drug was thawed 5 minutes before each treatment, serially diluted to the desired concentrations in media warmed to 37°C, and dispensed into microchambers in 3 sequential VRs followed by aspiration of the outlet port to reach desired final concentrations. LIVE/DEAD Viability/Cytotoxicity Assay Kit from Invitrogen was used to detect live and dead cells in microchambers. Both calcein AM (green) and ethidium homodimer (red) were used at a working concentration of 4µM.

Proteasome Activity Assay

Chymotryptic proteasomal activity was measured using the Proteasome-Glo Assay (Promega, Inc). RPMI8226 MM cells (5,000 per well), were plated in a white-walled 384-well tissue culture dish, allowed to rest for a minimum of 3 hours, and treated with increasing doses of bortezomib for 105 minutes before addition of the luminescent reagent as directed by the manufacturer in order to establish a standard curve of inhibition of the proteasome by differing concentrations of bortezomib. Luminescence was read on a Perkin-Elmer ENSPIRE plate reader. Relative light units for the no drug control were designated 100% proteasome activity, and the ratio of relative light units for each dose of bortezomib over control was used to determine the percentage decrease in chymotryptic activity. In order to extrapolate the bortezomib concentration over time within MicroC^3 channels, 100 nM bortezomib in media was added to MicroC^3 at different timepoints from 0 hr to 24 hrs. The media was then extracted after those timepoints and used to treat the RPMI8226 cells at a 10-fold dilution for 105 minutes. The same protocol as above was followed in order to determine percent inhibition of the proteasome. This percent inhibition of the proteasome was used to extrapolate an approximate molar concentration of bortezomib. After conversion of the molar concentration of bortezomib to ng/mL, the approximate concentration of bortezomib within MicroC^3 over time was used to calculate an AUC (ng x time in hrs/mL).

Immunofluorescence image analysis

Cells were stained with LIVE/DEAD for 10 min, and washed with one VR of fresh media. All fluorescent images were taken with a Nikon Eclipse Ti inverted fluorescent microscope coupled to a Nikon DS-Qi1Mc CCD camera (Nikon Instruments Inc., Melville, NY, USA) at a magnification of 4x. Image analysis was performed in ImageJ with custom in-house algorithms and database management to count live and dead cells (J'experiment) [31].

Statistical Analysis

Monocultured live fraction responses to bortezomib were normalized to the monoculture 0 dose; *cis*-cocultured live fraction responses to bortezomib were normalized to the coculture 0 dose. The changes in live fractions as a response to 30 nM and 100 nM doses of bortezomib were calculated. The mean, standard deviation, median, interquartile range (IQR), and Otsu threshold [74] were calculated for both monoculture and *cis*-coculture responses in Matlab (MathWorks, Nattick, MA) and graphed using Origin (OriginLab, Northampton, MA).

Clustering analysis of ex vivo data

In order to automatically identify potential distinct subpopulations in an unsupervised fashion and with high discriminative power, *ex vivo* data were separated using both *k*-means clustering [75] and Gaussian mixture (GM) modeling [76] algorithms. We chose to compare both methods for robustness. In both methods, the data set is iteratively partitioned into *k* clusters by minimizing the within-cluster variance while maximizing the between-cluster variance. Clustering of the *ex vivo* response data was carried out using the Statistics Toolbox of Matlab (MathWorks, Nattick, MA). The degree of dimensionality (i.e., the numbers of clusters) was determined by a) maximizing the mean Silhouette index of the *k*-means clusters and by b) minimizing the Akaike and Bayesian information criterion (AIC and BIC, respectively) of the Gaussian mixture model.

Acknowledgements

Funding: NIH R01 CA155192 (SM, DJB, NSC), MMRF Senior Award (SM, NSC), T32 GM008688 (CP), T32 CA009135 (CP), P30 CA014520 (SM, DJB, NSC, SS, KK) and Trillium Fund (SM, NSC, DJB, CP). **Author contributions**: CP, NSC, EWKY, DJB, and SM designed research. CP, EWKY, and KC performed research. NSC contributed patient samples and chemical reagents. BT, SS, and KK performed statistical analyses. CP and BT analyzed data and generated figures. CP, BT and SM wrote and NSC, EWKY, SS, KK, FA and DJB edited the paper. The authors would also like to thank Theodore de Groot for helpful discussions and design assistance. We also thank all the patients who have donated their bone marrow samples to the study. **Competing interests**: DJB. has ownership interest in Bellbrook Laboratories LLC, Tasso, Inc, and Salus Discovery, LLC. CP has ownership interest in Lynx Biosciences, LLC. The remaining authors declare no competing financial interests. CP, EWKY, NSC, SM, and DJB are inventors of a patent currently pending for MicroC^3.

Conclusions

With a collaboration that crossed multiple disciplines, including biomedical engineering, cellular biology, medicine, and statistics, we developed a microfluidic *cis*-coculture assay, MicroC^3, capable of testing the chemosensitivity and chemoresistance of patient tumor cells in coculture with their own non-tumor companion cells. When the *ex vivo* responses of MM patients to bortezomib were compared between MicroC^3 and monoculture, we found two groups of responses in MicroC^3 which correctly identified all seventeen patients as either clinically responsive or non-responsive to bortezomib-containing therapies, while responses in monoculture could not be unambiguously be grouped. Our results suggest that MicroC^3 may have the potential to predict the therapeutic responses of MM patients to bortezomib and other MM drugs. Furthermore, this system may not only be useful for the study of MM disease but other haematological malignancies as well.

Notes and references

[1]Molecular Pharmacology Graduate Program, [2]Department of Oncology, [3]Department of Medicine, Section of Hematology/Oncology, [4]University of Wisconsin Carbone Cancer Center, [5]Department of Biomedical Engineering, [6]Department of Medical Physics, University of Wisconsin-Madison, Madison, WI, [7]Cellectar Biosciences, Inc., Madison, WI, [8]Department of Biostatistics and Medical Informatics, University of Wisconsin-Madison, Madison, WI

†Current address: Department of Mechanical and Industrial Engineering, University of Toronto, Canada.

† Electronic Supplementary Information (ESI) available: [details of any supplementary information available should be included here]. See DOI: 10.1039/b000000x/

References

1 S. Ugurel, D. Schadendorf, C. Pföhler, K. Neuber, A. Thoelke, J. Ulrich, A. Hauschild, K. Spieth, M. Kaatz, W. Rittgen, S. Delorme, W. Tilgen and U. Reinhold, *Clin. Cancer Res.*, 2006, **12**, 5454–63.

2 D. J. Samson, J. Seidenfeld, K. Ziegler and N. Aronson, *J. Clin. Oncol.*, 2004, **22**, 3618–30.

3 H. J. Burstein, P. B. Mangu, M. R. Somerfield, D. Schrag, D. Samson, L. Holt, D. Zelman and J. a Ajani, *J. Clin. Oncol.*, 2011, **29**, 3328–30.

4 B. P. Cortazar and B. E. Johnson, *J. Cl*, 1999, **17**, 1625–1631.

5 A. Palumbo and K. Anderson, *N Engl J Med*, 2011, **364**, 1046–1060.

6 W. M. Kuehl and P. L. Bergsagel, *J Clin Invest*, 2012, **122**.

7 S. K. Kumar, J. R. Mikhael, F. K. Buadi, D. Dingli, A. Dispenzieri, R. Fonseca, M. A. Gertz, P. R. Greipp, S. R. Hayman, R. A. Kyle, M. Q. Lacy, J. A. Lust, C. B. Reeder, V. Roy, S. J. Russell, K. E. Short, A. K. Stewart, T. E. Witzig, S. R. Zeldenrust, R. J. Dalton, S. V Rajkumar and P. L. Bergsagel, *Mayo Clin Proc*, 2009, **84**, 1095–1110.

8 R. Siegel, J. Ma, Z. Zou and A. Jemal, *CA Cancer J Clin*, 2014, **64**, 9–29.

9 S. Vincent Rajkumar, *Am. J. Hematol.*, 2013, **88**, 225–235.

10 H. Ludwig and P. Sonneveld, *Leuk Res*, 2012, **36 Suppl 1**, S27–34.

11 P. Richardson, C. Mitsiades, R. Schlossman, I. Ghobrial, T. Hideshima, D. Chauhan, N. Munshi and K. Anderson, *Hematol. Am Soc Hematol Educ Progr.*, 2007, 317–323.

12 K. Fostier, A. De Becker and R. Schots, *Onco Targets Ther*, 2012, **5**, 237–244.

13 S. Sinha, M. Lacy, J. Mikhael, S. Hayman, F. Buadi, K. Detweiler-Short, A. Dispenzieri, M. Gertz, D. Dingli, S. V Rajkumar and S. K. Kumar, *Leukemia*, 2012, **26**, 839–841.

14 T. Hideshima, C. Mitsiades, G. Tonon, P. G. Richardson and K. C. Anderson, *Nat Rev Cancer*, 2007, **7**, 585–598.

15 S. Markovina, N. S. Callander, S. L. O'Connor, G. Xu, Y. Shi, C. P. Leith, K. Kim, P. Trivedi, J. Kim, P. Hematti and S. Miyamoto, *Mol Cancer*, 2010, **9**, 176.

16 F. Asimakopoulos, J. Kim, R. A. Denu, C. Hope, J. L. Jensen, S. J. Ollar, E. Hebron, C. Flanagan, N. Callander and P. Hematti, *Leuk Lymphoma*, 2013, **54**, 2112–2121.

17 C. Hope, S. J. Ollar, E. Heninger, E. Hebron, J. L. Jensen, J. Kim, I. Maroulakou, S. Miyamoto, C. Leith, D. T. Yang, N. Callander, P. Hematti, M. Chesi, P. L. Bergsagel and F. Asimakopoulos, *Blood*, 2014.

18 J. Kim, R. A. Denu, B. A. Dollar, L. E. Escalante, J. P. Kuether, N. S. Callander, F. Asimakopoulos and P. Hematti, *Br J Haematol*, 2012, **158**, 336–346.

19 D. Gupta, S. P. Treon, Y. Shima, T. Hideshima, K. Podar, Y. T. Tai, B. Lin, S. Lentzsch, F. E. Davies, D. Chauhan, R. L. Schlossman, P. Richardson, P. Ralph, L. Wu, F. Payvandi, G. Muller, D. I. Stirling and K. C. Anderson, *Leukemia*, 2001, **15**, 1950–1961.

20 G. Bianchi and I. M. Ghobrial, *Leuk. Lymphoma*, 2013, **54**, 229–241.

21 M. Ferrarini, N. Steimberg, M. Ponzoni, D. Belloni, A. Berenzi, S. Girlanda, F. Caligaris-Cappio, G. Mazzoleni and E. Ferrero, *PLoS One*, 2013, **8**, e71613.

22 Z. P. Khin, M. L. C. Ribeiro, T. Jacobson, L. Hazlehurst, L. Perez, R. Baz, K. Shain and A. S. Silva, *Cancer Res.*, 2014, **74**, 56–67.

23 T. Calimeri, E. Battista, F. Conforti, P. Neri, M. T. Di Martino, M. Rossi, U. Foresta, E. Piro, F. Ferrara, a Amorosi, N. Bahlis, K. C. Anderson, N. Munshi, P. Tagliaferri, F. Causa and P. Tassone, *Leukemia*, 2011, **25**, 707–11.

24 J. Kirshner, K. J. Thulien, L. D. Martin, C. Debes Marun, T. Reiman, A. R. Belch and L. M. Pilarski, *Blood*, 2008, **112**, 2935–45.

25 A. L. Paguirigan, J. P. Puccinelli, X. Su and D. J. Beebe, *Assay Drug Dev Technol*, 2010, **8**, 591–601.

26 E. W. Young and D. J. Beebe, *Chem Soc Rev*, 2010, **39**, 1036–1048.

27 R. N. Zare and S. Kim, *Annu Rev Biomed Eng*, 2010, **12**, 187–201.

28 R. Cheong, C. J. Wang and A. Levchenko, *Sci Signal*, 2009, **2**, pl2.

29 G. Walker and D. J. Beebe, *Lab Chip*, 2002, **2**, 131–134.

30 X. Li, D. R. Ballerini and W. Shen, *Biomicrofluidics*, 2012, **6**, 11301–1130113.

31 E. W. Young, C. Pak, B. S. Kahl, D. T. Yang, N. S. Callander, S. Miyamoto and D. J. Beebe, *Blood*, 2012, **119**, e76–85.

32 S. Markovina, N. S. Callander, S. L. O'Connor, J. Kim, J. E. Werndli, M. Raschko, C. P. Leith, B. S. Kahl, K. Kim and S. Miyamoto, *Mol Cancer Res*, 2008, **6**, 1356–1364.

33 D. Chen, M. Frezza, S. Schmitt, J. Kanwar and Q. Dou, *Curr Cancer Drug Targets*, 2012, **11**, 239–253.

34 Z. J. Gu, J. De Vos, C. Rebouissou, M. Jourdan, X. G. Zhang, J. F. Rossi, J. Wijdenes and B. Klein, *Leukemia*, 2000, **14**, 188–197.

35 J. De Vos, C. Bagnis, L. Bonnafoux, G. Requirand, M. Jourdan, M.-C. Imbert, E. Jourdan, J.-F. Rossi, P. Mannoni and B. Klein, *Hum. Gene Ther.*, 2003, **14**, 1727–39.

36 D. E. Reece, D. Sullivan, S. Lonial, A. F. Mohrbacher, G. Chatta, C. Shustik, H. Burris, K. Venkatakrishnan, R. Neuwirth, W. J. Riordan, M. Karol, L. L. von Moltke, M. Acharya, P. Zannikos and a Keith Stewart, *Cancer Chemother. Pharmacol.*, 2011, **67**, 57–67.

37 P. Moreau, H. Pylypenko, S. Grosicki, I. Karamanesht, X. Leleu, M. Grishunina, G. Rekhtman, Z. Masliak, T. Robak, A. Shubina, B. Arnulf, M. Kropff, J. Cavet, D.-L. Esseltine, H. Feng, S. Girgis, H. van de Velde, W. Deraedt and J.-L. Harousseau, *Lancet. Oncol.*, 2011, **12**, 431–40.

38 B. G. M. Durie, J.-L. Harousseau, J. S. Miguel, J. Bladé, B. Barlogie, K. Anderson, M. Gertz, M. Dimopoulos, J. Westin, P. Sonneveld, H. Ludwig, G. Gahrton, M. Beksac, J. Crowley, a Belch, M. Boccadaro, M. Cavo, I. Turesson, D. Joshua, D. Vesole, R. Kyle, R. Alexanian, G. Tricot, M. Attal, G. Merlini, R. Powles, P. Richardson, K. Shimizu, P. Tosi, G. Morgan and S. V Rajkumar, *Leukemia*, 2006, **20**, 1467–73.

39 R. Fonseca, E. Blood, D. Harrington, M. M. Oken, R. A. Kyle, G. W. Dewald, B. Van Ness, S. A. Van Wier, K. J. Henderson, R. J. Bailey and P. R. Greipp, 2003, **101**, 4569–4575.

40 B. Nair, F. van Rhee, J. D. Shaughnessy, E. Anaissie, J. Szymonifka, A. Hoering, Y. Alsayed, S. Waheed, J. Crowley and B. Barlogie, *Blood*, 2010, **115**, 4168–73.

41 R. Fonseca, P. L. Bergsagel, J. Drach, J. Shaughnessy, N. Gutierrez, a K. Stewart, G. Morgan, B. Van Ness, M. Chesi, S. Minvielle, a Neri, B. Barlogie, W. M. Kuehl, P. Liebisch, F. Davies, S. Chen-Kiang, B. G. M. Durie, R. Carrasco, O. Sezer, T. Reiman, L. Pilarski and H. Avet-Loiseau, *Leukemia*, 2009, **23**, 2210–21.

42 D. Chauhan, H. Uchiyama, Y. Akbarali, M. Urashima, K. Yamamoto, T. A. Libermann and K. C. Anderson, *Blood*, 1996, **87**, 1104–1112.

43 A. M. Roccaro, T. Hideshima, N. Raje, S. Kumar, K. Ishitsuka, H. Yasui, N. Shiraishi, D. Ribatti, B. Nico, A. Vacca, F. Dammacco, P. G. Richardson and K. C. Anderson, *Cancer Res*, 2006, **66**, 184–191.

44 U. Heider, M. Kaiser, C. Müller, C. Jakob, I. Zavrski, C. O. Schulz, C. Fleissner, M. Hecht and O. Sezer, *Eur. J. Haematol.*, 2006, **77**, 233–238.

45 M. R. Junttila and F. J. de Sauvage, *Nature*, 2013, **501**, 346–354.

46 P. L. Bedard, A. R. Hansen, M. J. Ratain and L. L. Siu, *Nature*, 2013, **501**, 355–364.

47 E. Leich, S. Weißbach, H.-U. Klein, T. Grieb, J. Pischimarov, T. Stühmer, M. Chatterjee, T. Steinbrunn, C. Langer, M. Eilers, S. Knop, H. Einsele, R. Bargou and a Rosenwald, *Blood Cancer J.*, 2013, **3**, e102.

48 G. Misso, S. Zappavigna, M. Castellano, G. De Rosa, M. T. Di Martino, P. Tagliaferri, P. Tassone and M. Caraglia, *Expert Opin. Biol. Ther.*, 2013, **13**, S95–S109.

49 M. Domenech, H. Yu, J. Warrick, N. M. Badders, I. Meyvantsson, C. M. Alexander and D. J. Beebe, *Integr. Biol. (Camb).*, 2009, **1**, 267–74.

50 E. K. Sackmann, A. L. Fulton and D. J. Beebe, *Nature*, 2014, **507**, 181–189.

51 S. Takayama, J. C. McDonald, E. Ostuni, M. N. Liang, P. K. Kenis, R. F. Ismagilov and G. M. Whitesides, *Proc. Natl. Acad. Sci. U. S. A.*, 1999, **96**, 5545–5548.

52 Y.-S. Torisawa, B. Mosadegh, T. Bersano-Begey, J. M. Steele, K. E. Luker, G. D. Luker and S. Takayama, *Integr. Biol. (Camb).*, 2010, **2**, 680–6.

53 E. W. K. Young, *Integr. Biol. (Camb).*, 2013, **5**, 1096–109.

54 A. M. Taylor, S. W. Rhee, C. H. Tu, D. H. Cribbs and C. W. Cotman, *Langmuir*, 2010, **19**, 1551–1556.

55 T. H. Lippert, H.-J. Ruoff and M. Volm, *Int. J. Med. Sci.*, 2011, **8**, 245–53.

56 M. Suggitt and M. C. Bibby, *Clin Cancer Res*, 2005, **11**, 971–981.

57 J. Laubach, T. Hideshima, P. Richardson and K. Anderson, *Semin Oncol*, 2013, **40**, 549–553.

58 S. V. Rajkumar, *Am. J. Hematol.*, 2014, **89**, 837–851.

59 R. Z. Khan and A. Badros, *Expert Rev Hematol*, 2012, **5**, 361–372.

60 K. C. Anderson, *J Natl Compr Canc Netw*, 2013, **11**, 676–679.

61 L. J. Crawford, B. Walker and A. E. Irvine, *J. Cell Commun. Signal.*, 2011, **5**, 101–10.

62 Y. X. Zhu, K. M. Kortuem and A. K. Stewart, *Leuk Lymphoma*, 2013, **54**, 683–687.

63 G. Lu, R. E. Middleton, H. Sun, M. Naniong, C. J. Ott, C. S. Mitsiades, K.-K. Wong, J. E. Bradner and W. G. Kaelin, *Science*, 2013, **305**.

64 M. Bolzoni, P. Storti, S. Bonomini, K. Todoerti, D. Guasco, D. Toscani, L. Agnelli, A. Neri, V. Rizzoli and N. Giuliani, *Exp Hematol*, 2013, **41**, 387–397 e1.

65 J. Krönke, N. D. Udeshi, A. Narla, P. Grauman, S. N. Hurst, M. McConkey, T. Svinkina, D. Heckl, E. Comer, X. Li, C. Ciarlo, E. Hartman, N. Munshi, M. Schenone, S. L. Schreiber, S. a Carr and B. L. Ebert, *Science*, 2013, **301**.

66 C. S. Mitsiades, *Blood*, 2011, 117, 1440–1441.

67 F.-M. Zi, J.-S. He, Y. Li, C. Wu, W.-J. Wu, Y. Yang, L.-J. Wang, D.-H. He, L. Yang, Y. Zhao, G.-F. Zheng, X.-Y. Han, H. Huang, Q. Yi and Z. Cai, *Cancer Biol. Ther.*, 2014, **15**, 1–10.

68 M. Ferrarini, G. Mazzoleni, N. Steimberg, D. Belloni and E. Ferrero, in *InTech*, 2013, pp. 39–60.

69 J. Schüler, D. Ewerth, J. Waldschmidt, R. Wäsch and M. Engelhardt, *Expert Opin. Biol. Ther.*, 2013, **13 Suppl 1**, S111–23.

70 Y. Torisawa, C. S. Spina, T. Mammoto, A. Mammoto, J. C. Weaver, T. Tat, J. J. Collins and D. E. Ingber, *Nat. Methods*, 2014.

71 M. Hidalgo, F. Amant, a. V. Biankin, E. Budinska, a. T. Byrne, C. Caldas, R. B. Clarke, S. de Jong, J. Jonkers, G. M. Maelandsmo, S. Roman-Roman, J. Seoane, L. Trusolino and a. Villanueva, *Cancer Discov.*, 2014.

72 Y. Xia and G. M. Whitesides, *Annu. Rev. Mater. Sci.*, 1998, 28, 153–184.

73 Duffy, J. McDonald, O. Schueller and G. Whitesides, *Anal. Chem*, 1998, **70**, 4974–4984.

74 T. Kurita, N. Otsu and N. Abdelmalek, *Pattern Recognit.*, 1992, 25, 1231–1240.

75 J. a Hartigan and M. a Wong, *J. R. Stat. Soc.*, 1979, **28**, 100–108.

76 G. McLachlan and D. Peel, *Finite Mixture Models*, 2000, vol. 44.